International Journal of Electrical, Electronic and Communication Sciences
ISSN: 2517-9438
Vol:9, No:8, 2015

Comparative Dynamic Performance of Load Frequency Control of Nonlinear Interconnected Hydro-Thermal System Using Intelligent Techniques

Banaja Mohanty, Prakash Kumar Hota

***Abstract*—**This paper demonstrates dynamic performance evaluation of load frequency control (LFC) with different intelligent techniques. All non-linearities and physical constraints have been considered in simulation studies such as governor dead band (GDB), generation rate constraint (GRC) and boiler dynamics. The conventional integral time absolute error has been considered as objective function. The design problem is formulated as an optimisation problem and particle swarm optimisation (PSO), bacterial foraging optimisation algorithm (BFOA) and differential evolution (DE) are employed to search optimal controller parameters. The superiority of the proposed approach has been shown by comparing the results with published fuzzy logic control (FLC) for the same interconnected power system. The comparison is done using various performance measures like overshoot, undershoot, settling time and standard error criteria of frequency and tie-line power deviation following a step load perturbation (SLP). It is noticed that, the dynamic performance of proposed controller is better than FLC. Further, robustness analysis is carried out by varying the time constants of speed governor, turbine, tie-line power in the range of +40% to -40% to demonstrate the robustness of the proposed DE optimized PID controller.

***Keywords*—**Automatic generation control, governor dead band, generation rate constraint, differential evolution.

I. Introduction

LFC is an important issue in power system operation and control. Large power systems are divided into different control areas. All such areas are connected, to be called as an interconnected power system. Interconnected power system is used to increase reliable and uninterrupted power supply. Normally, in interconnected power systems, either thermal-thermal or hydro-thermal type systems are considered. Automatic generation control (AGC) is used to maintain the scheduled system frequency and tie line power deviations in case of normal operation as well as small perturbation. AGC function can be viewed as a supervisory control function which attempts to match the generation trend within an area to the trend of the randomly changing load of the same and different areas, so as to keep the system frequency and the tie-line power flow close to the scheduled values. The growth in size and complexity of electric power systems along with increase in power demand has necessitated the use of intelligent systems that combine knowledge, techniques and methodologies from various sources for the real-time control of power systems. Kothari et al. [1] are possibly the first to consider GRC to investigate the AGC problem of a hydro-thermal system with conventional integral controllers. Many a research has been done in AGC for two area thermal -hydro systems with non-linearity as GRC [2], [3]. In [4], GDB is considered as non-linearity, and the AGC problem is solved by PI controller tuned with craziness particle swarm optimisation (CPSO).

It is observed that, considerable research work is still going on to propose better AGC systems based on modern control theory [5], neural network [6], fuzzy system theory [7], reinforcement learning [8] and ANFIS approach [9], etc. But, these advanced approaches are complicated and need familiarity of users to these techniques, thus reducing their applicability. Alternatively, a classical proportional-integral (PI) and proportional integral derivative (PID) controllers remain an engineer's preferred choice due to its structural simplicity, reliability and the favourable ratio between performances and cost. Additionally, it also offers simplified dynamic modelling, lower user-skill requirements and minimal development as effort, which are the major issues of in engineering practice.

In recent times, new artificial intelligence-based approaches have been proposed to optimize the PI/PID controller parameters for AGC system. In [10], several classical controller structures such as Integral (I), PI, integral derivative (ID), PID and integral double derivative (IDD) have been applied and their performance have been compared for an AGC system with BFOA. Nanda et al. [11] have demonstrated that BFOA optimized controller provides better performance than GA based controllers and conventional controllers for an interconnected power system. In [12], a modified objective function using Integral of Time multiplied by Absolute value of Error (ITAE), damping ratio of dominant eigenvalues and settling time is proposed where, the PI controller parameters are optimized employing DE algorithm, and the results are compared with BFOA and GA optimized based PI controller to show its superiority. Anand et al. [13] have reported a conventional PI controller with FLC for stabilising the frequency oscillations of AGC with nonlinearities.

DE is a population-based direct search algorithm for global optimization which is capable of handling non-differentiable, non-linear and multi-modal objective functions with few

B.Mohanty is with the Electrical Engineering Department Veer Surendra Sai University of Technology, Burla, India (phone: 91-9437152730; e-mail: banaja_m@yahoo.com).

P.K. Hota is Professor with Electrical Engineering Department Veer Surendra Sai University of Technology, Burla (e-mail: p_hota@rediffmail.com).

easily chosen control parameters [14]. DE uses weighted differences between solution vectors to change the population whereas, in other stochastic techniques such as Genetic Algorithm (GA) and Expert Systems (ES), perturbation occurs in accordance with a random quantity. DE employs a greedy selection process with inherent elitist features. Also, it has a minimum number of control parameters, which can be tuned effectively [15].

In view of the above, an attempt has been made in this paper for the optimal design of DE based classical PI/PID controllers for LFC of multi-area linear and nonlinear interconnected power system. The design problem of the proposed controller is formulated as an optimization problem and DE is employed to search for optimal controller parameters. Simulations results are presented to show the effectiveness of the presented controller in providing good damping characteristics to system oscillations over a wide range of disturbances. Further, the superiority of the proposed design approach is illustrated by comparing the presented approach with recently published conventional as PI controller and FLC [13] for the same AGC system.

II. System Modeling

The block diagram model of two areas interconnected hydro-thermal system with nonlinearities and boiler dynamics are shown in Fig. 1. Thermal area comprised of reheat turbine, GDB, GRC and boiler dynamics. The hydro area also incorporated GDB and GRC.

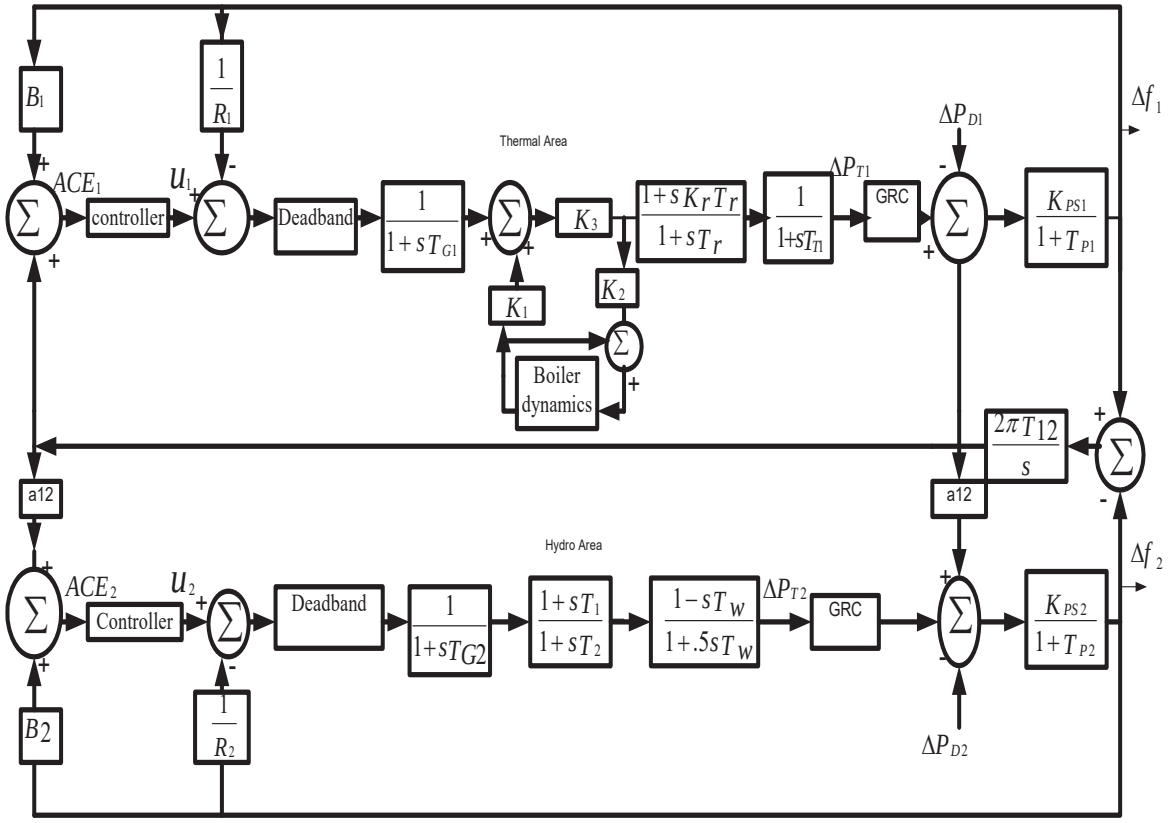

Fig. 1 Transfer function model of two area hydro-thermal system with boiler dynamics, GDB and GRC

In Fig. 1, B_1 and B_2 are the frequency bias parameters; ACE_1 and ACE_2 are area control errors; u_1 and u_2 are the control outputs form the controller; R_1 and R_2 are the governor speed regulation parameters in pu Hz; T_{G1} and T_{G2} are the speed governor time constants in sec; ΔP_{G1} and ΔP_{G2} are the change in governor valve positions (pu); T_{T1} and T_{T2} are the turbine time constant in sec; K_r and Tr are the gain and time constant of reheat turbine; ΔP_{D1} and ΔP_{D2} are the load demand changes; ΔP_{tie} is the incremental change in tie line power (p.u); K_{P1} and K_{P2} are the power system gains; T_{P1} and T_{P2} are the power system time constant in sec; T_{12} is the synchronizing coefficient and Δf_1 and Δf_2 are the system frequency deviations in Hz,. The relevant parameters are given in appendix.

GDB is defined as the total magnitude of a sustained speed change within which there is no resulting change in valve position. The backlash non-linearity tends to produce a continuous sinusoidal oscillation with a natural period of about 2 s. The speed GDB has significant effect on the dynamic performance of LFC mechanism. For this analysis, in this study backlash non-linearity of about 0.05% for thermal system and the dead band non-linearity of about 0.02% for hydro system are considered. The system is provided with a

single reheat turbine with an appropriate GRC of 0.0017MW per sec for thermal area and 4.5% per sec for rising generation and 6% for lowering generation for hydro area as shown in Fig. 2.

Boiler is a device for producing steam under pressure. In this study, the effect of the boiler in steam area in the power system is also considered and detailed configuration is shown in Fig. 3 which is adopted from [13]. This includes the long term dynamics of fuel and steam flow on boiler drum pressure. Representations for combustion controls are also incorporated. This model is basically a normally used drum type boiler and fuel used is oil/gas. The model can be used to study the responses of coal fired units with poorly tuned (oscillatory) combustion controls, coal fired units with well tuned controls and well tuned oil or gas fired units.

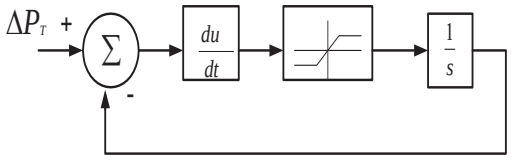

Fig. 2 GRC

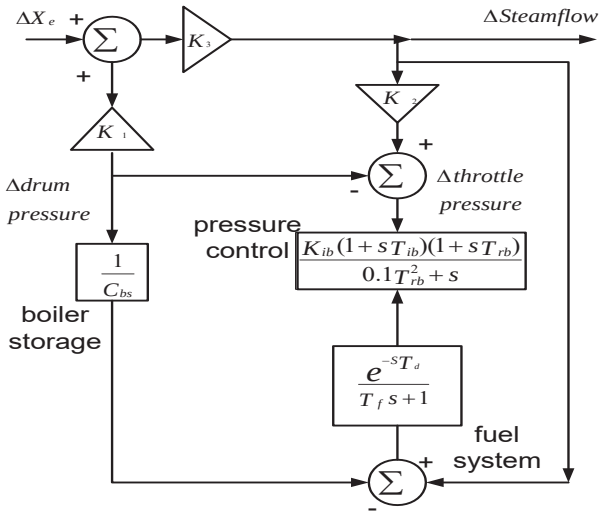

Fig. 3 Boiler dynamics

III. The Proposed Approach

PID controller is the most popular feedback controller used in the process industries. It is a robust, easily understood controller that can provide excellent control performance despite the varied dynamic characteristics of process plant. As the name suggests, the PID algorithm consists of three basic modes, the proportional mode, the integral and the derivative modes. A proportional controller has the effect of reducing the rise time, but never eliminates the steady-state error. An integral control has the effect of eliminating the steady-state error, but it may make the transient response worse. A derivative control has the effect of increasing the stability of the system i.e., reducing the overshoot and improving the transient response. PI controllers are the most often used controller today in industry. A control without derivative (D) mode is used when: Fast response of the system is not required, large disturbances and noises are present during operation of the process and there are large transport delays in the system. Derivative mode improves stability of the system and enables increase in proportional gain and decrease in integral gain which in turn increases speed of the controller response. PID controller is often used when stability and fast response are required. On the other hand, design of a fuzzy based controller requires more design decision than usual, for example, regarding the number of membership functions, their shape, and their overlap for all inputs and outputs, rule base, inference engine, defuzzification, and data pre and post processing. Therefore, fuzzy logic based controllers suffer from the requirement of expert user in their design and implementation, and mathematical rigors and so are vulnerable to the experts' depth of knowledge in problem definition. In view of the above, both PI and PID structured controllers are considered in the present work. Design of PID controller requires determination of the three main parameters, proportional gain (K_P), integral time constant (K_I) and derivative time constant (K_D). For PI controller K_P and K_I are to be determined. The controllers in both the areas are considered to be different and so that they are K_{P1}, $K_{P2}K_{I1}$, K_{I2} and K_{D1}, K_{D2}.

The error inputs to the controllers are the respective area control errors (ACE) are given by:

$$e_1(t) = ACE_1 = B_1\Delta f_1 + \Delta P_{Tie} \quad (1)$$

$$e_2(t) = ACE_2 = B_2\Delta f_2 - \Delta P_{Tie} \quad (2)$$

The control inputs of the power system u_1 and u_2 with PI structure are obtained as:

$$u_1 = K_{P1}ACE_1 + K_{I1}\int ACE_1 \quad (3)$$

$$u_2 = K_{P2}ACE_2 + K_{I2}\int ACE_2 \quad (4)$$

The control inputs of the power system u_1 and u_2 with PID structure are obtained as

$$u_1 = K_{P1}ACE_1 + K_{I1}\int ACE_1 + K_{D1}\frac{dACE_1}{dt} \quad (5)$$

$$u_2 = K_{P2}ACE_2 + K_{I2}\int ACE_2 + K_{D2}\frac{dACE_2}{dt} \quad (6)$$

In the design of a PI/PID controller, the objective function is first defined based on the desired specifications and constraints. The design of objective function to tune the controller is generally based on a performance index that considers the entire closed loop response. Typical output specifications in the time domain are peak overshoot, rise

time, settling time and steady-state error. The following four kinds of performance criteria are considered in the control design namely the Integral of Time multiplied Absolute Error (ITAE), Integral of Squared Error (ISE), Integral of Time multiplied Squared Error (ITSE) and Integral of Absolute Error (IAE). The objective function considered in this case is given below:

$$J_1 = ISE = \int_0^{t_{sim}} (\Delta f_1)^2 + (\Delta f_2)^2 + (\Delta P_{Tie})^2 \cdot dt \quad (7)$$

where, Δf_1 and Δf_2 are the system frequency deviations; ΔP_{Tie} is the incremental change in tie line power; t_{sim} is the time range of simulation.

Minimize J
Subject to
$K_{P\min} \le K_P \le K_{P\max}$ *and* $K_{I\min} \le K_I \le K_{I\max}$

As reported, the minimum and maximum values of controller parameters are chosen as 0 and 3 respectively.

IV. Intelligent Techniques

A. PSO

PSO method is a member of wide category of Swarm Intelligence methods for solving the optimization problems. It is a population based search algorithm where each individual is referred to as particle and represents a candidate solution. Each particle in PSO flies through the search space with an adaptable velocity that is dynamically modified according to its own flying experience and also the flying experience of the other particles. In PSO each particles strive to improve themselves by imitating traits from their successful peers. Further, each particle has a memory and hence it is capable of remembering the best position in the search space ever visited by it. The position corresponding to the best fitness is known as pbest and the overall best out of all the particles in the population is called gbest. The modified velocity and position of each particle can be calculated using the current velocity and the distance from the pbest j,g to gbestg as shown in:

$$v_{f,g}^{(t+1)} = w * v_{j,g}^{(t)} + c_1 * r_1() * (pbest_{j,g} - x_{j,g}^{(t)}) + \quad c_2 * r_2() * (gbest_g - x_{j,g}^{(t)}) \quad (8)$$

$$x_{f,g}^{(t+1)} = x_{j,g}^{(t)} + v_{j,g}^{(t+1)} \quad (9)$$

with j = 1, 2... n and g = 1,2...m where n =number of particles in a group; m = number of members in a particle; t = number of iterations (generations); $v_{j,g}^{(t)}$ = velocity of particle j at iteration t, with $v_g^{\min} \le v_{j,g}^{(t)} \le v_g^{\max}$ c1, c2 = cognitive and social acceleration factors respectively; r1, r2 = random numbers uniformly distributed in the range (0, 1); $x_{j,g}^{(t)}$ = Current position of j at iteration t; Pbest j = pbest of particle j;gbest = gbest of the group.

The j-th particle in the swarm is represented by a g-dimensional vector xj = (xj,1, xj,2, ……,xj,g) and its rate of position change (velocity) is denoted by another g-dimensional vector vj = (vj,1, vj,2, ……, vj,g). The best previous position of the j-th particle is represented as pbestj = (pbestj, 1, pbestj, 2… pbestj, g). The index of best particle among all of the particles in the group is represented by the gbestg.

In PSO, each particle moves in the search space with a velocity according to its own previous best solution and its group's previous best solution. The velocity update in a PSO consists of three parts; namely momentum, cognitive and social parts. The balance among these parts determines the performance of a PSO algorithm. The parameters c1 & c2 determine the relative pull of pbest and gbest and the parameters r1 & r2 help in stochastically varying these pulls. In the above equations, superscripts denote the iteration number. The computational flow chart of PSO algorithm is shown in Fig. 2.

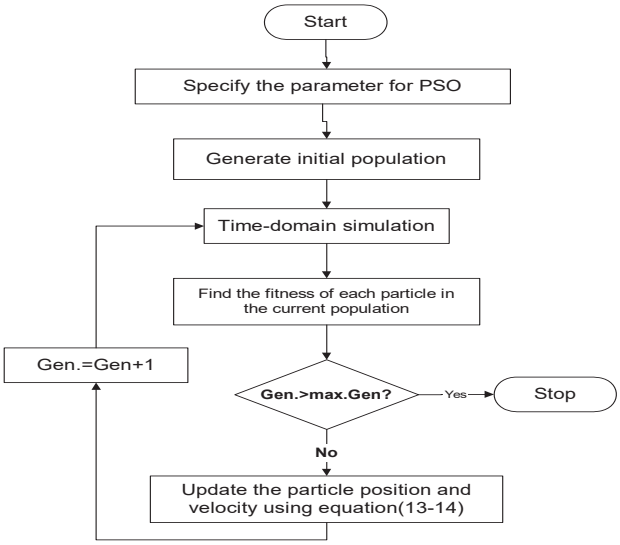

Fig. 4 Flowcharts of particle swarm optimization algorithm

B. BFOA

Application of group foraging strategy of a swarm of *E. coli* bacteria in multi-optimal function optimization is the idea behind BFOA. The foraging behavior of *E. coli* bacteria present in our intestines includes the methods of locating, handling and ingesting food, has been successfully mimicked in BFOA. Each bacterium tries to maximize its obtained energy per each unit of time expended on the foraging process and avoids noxious substances. Further, individual bacterium communicates with other individuals by sending signals.

The optimization technique consists of determining the minimum of a function $J(\alpha)$ where the variables under consideration constitute the high-dimensional vector $\alpha \in \Re p$ and it is very difficult or almost impossible to determine $\delta J(\alpha)$. Here, α determines the position of a bacterium in high

dimensional space. A negative value of $J(\alpha)$ indicates that the bacterium is in nutrient-rich environment, a zero value indicates a neutral environment and a positive value indicates a noxious environment. The objective will be to try and implement a biased random walk for each bacterium where it will try to climb up the nutrient concentration and, try and avoid noxious substances and will attempt to leave a neutral environment as soon as possible. This optimization procedure comprises of four basic steps: Swarming and tumbeling Chemotaxis, Reproduction and Elimination and, Dispersal [11], [15], [16].

1) Swarming and Tumbling via Flagella (N_S)

During foraging of the bacteria, locomotion is realized by a set of tensile flagella. An *E. coli* bacterium can move in two different ways; it can swim for a period of time or it can tumble. When they rotate the flagella in the clockwise direction, each flagellum pulls on the cell, which results in the moving of flagella independently and finally the bacterium tumbles with lesser number of tumbling. In a harmful place it tumbles frequently to find a nutrient gradient. Moving the flagella in the counterclockwise direction helps the bacterium to swim at a very fast rate. The bacterium alternates between these two modes of operation its entire lifetime. The cell-to-cell signaling in *E. coli* swarm may be represented by:

$$J_C(\alpha, P(j,k,l)) = \sum_{i=1}^{N} J_C(\alpha, \alpha^i(j,k,l))$$
$$= \sum_{i=1}^{N}[-d_{at}\exp(-w_{at}\sum_{m=1}^{P}(\alpha_m - \alpha_m^i)^2)] + \sum_{i=1}^{N}[h_{re}\exp(-w_{re}\sum_{m=1}^{P}(\alpha_m - \alpha_m^i)^2)] \quad (10)$$

$J_C(\alpha, P(j,k,l))$ is the objective function value which is to be added to the actual objective function to get a time varying objective function, N is the total number of bacteria, P is the number of variables to be optimized, $\alpha = [\alpha_1, \alpha_2, \ldots \alpha_P]^T$ is a point in the P-dimensional search domain and $d_{at}, w_{at}, h_{re}, w_{re}$ are different attractant and repellant coefficients.

1) Chemotaxis (N_C)

Chemotaxis process simulates the movement of an *E. coli* cell through swimming and tumbling via flagella. Suppose $\alpha^i(j,k,l)$ represents i-th bacterium at j-th chemotactic, k-th reproductive and l-th elimination-dispersal step, and then in computational chemotaxis the movement of the bacterium may be represented by:

$$\alpha^i(j+1,k,l) = \alpha^i(j,k,l) + S(i)\frac{\delta(i)}{\sqrt{\delta^T(i)\delta(i)}} \quad (11)$$

where, $S(i)$ is the size of the step taken in the random direction specified by the tumble (run length unit) and δ indicates a vector in the random direction in the range (-1, 1).

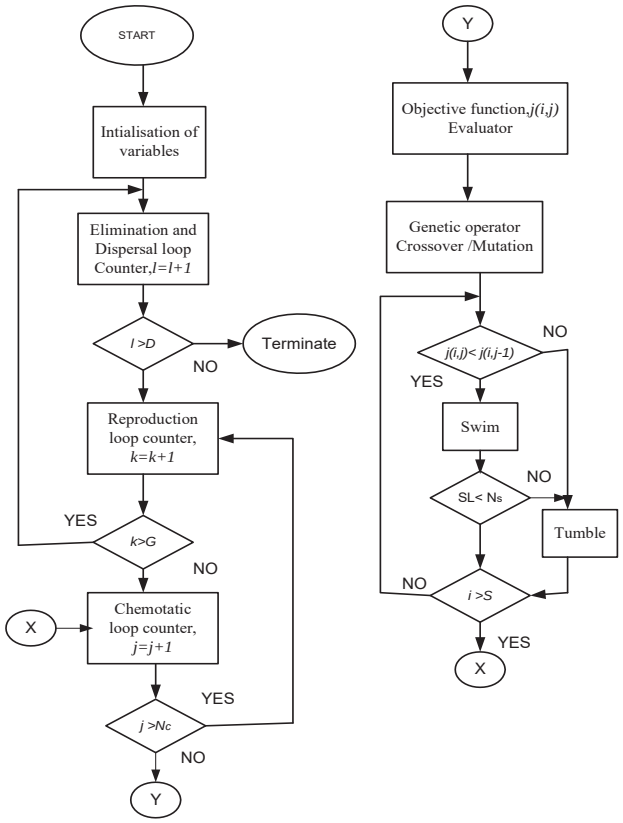

Fig. 5 Flow chart of BFOA

2) Reproduction (N_{re})

In this process, the least healthy bacteria eventually die while each of the healthier bacteria giving better objective function values asexually split into two bacteria. These new bacteria are placed in the same location to keep the swarm size constant.

3) Elimination and Dispersal (N_{ed})

Gradual or sudden changes in the local environment where a bacterium population lives may occur due to various reasons. When local significant increase in heat kills a population of bacteria that are currently in a region with a high concentration of nutrient gradients is called the elimination process. A sudden flow of water can disperse bacteria from one place to another. Elimination and dispersal events may destroy chemotactic progress, but they also have the effect of assisting in chemotaxis, since dispersal may place bacteria near good food sources. To simulate this phenomenon in BFOA some bacteria are liquidated at random with a very small probability while the new replacements are randomly initialized over the search space. The flow chart of BFOA is given in Fig. 5.

C. DE

DE algorithm is a population-based stochastic optimization algorithm recently introduced [14]. Advantages of DE are: simplicity, efficiency & real coding, easy use, local searching property and speediness. DE works with two populations; old

generation and new generation of the same population. The size of the population is adjusted by the parameter N_P. The population consists of real valued vectors with dimension D that equals the number of design parameters/control variables. The population is randomly initialized within the initial parameter bounds. The optimization process is conducted by means of three main operations: mutation, crossover and selection. In each generation, individuals of the current population become target vectors. For each target vector, the mutation operation produces a mutant vector, by adding the weighted difference between two randomly chosen vectors to a third vector. The crossover operation generates a new vector, called trial vector, by mixing the parameters of the mutant vector with those of the target vector. If the trial vector obtains a better fitness value than the target vector, then the trial vector replaces the target vector in the next generation. The evolutionary operators are described below [17], [18].

1) Initialization

For each parameter j with lower bound x_j^L and upper bound x_j^U, initial parameter values are usually randomly selected uniformly in the interval [x_j^L , x_j^U].

2) Mutation

For a given parameter vector $X_{i,G}$, three vectors ($X_{r1,G}$ $X_{r2,G}$ $X_{r3,G}$) are randomly selected such that the indices i, $r1$, $r2$ and $r3$ are distinct. A donor vector $V_{i,G+1}$ is created by adding the weighted difference between the two vectors to the third vector as:

$$V_{i,G+1} = X_{r1,G} + F(X_{r2,G} - X_{r3,G}) \tag{12}$$

where, F is a constant within the range (0, 2) and denotes generation.

3) Crossover

Three parents are selected for crossover and the child is a perturbation of one of them. The trial vector $U_{i,G+1}$ is developed from the elements of the target vector ($X_{i,G}$) and the elements of the donor vector ($X_{i,G}$). Elements of the donor vector enters the trial vector with probability CR as:

$$U_{j,i,G+1} = \begin{cases} V_{j,i,G+1} & if \quad rand_{j,i} \le CR \quad or \quad j = I_{rand} \\ X_{j,i,G+1} & if \quad rand_{j,i} > CR \quad or \quad j \ne I_{rand} \end{cases} \tag{13}$$

where $rand_{j,i} \sim U(0,1)$, I_{rand} is a random integer from $(1,2,.....D)$ and D is the solution's dimension i.e. number of control variables. I_{rand} ensures that $V_{i,G+1} \ne X_{i,G}$.

4) Selection

The target vector $X_{i,G}$ is compared with the trial vector $V_{i,G+1}$ and the one with the better fitness value is admitted to the next generation. The selection operation in DE can be represented by:

$$X_{i,G+1} = \begin{cases} U_{i,G+1} & if \quad f(U_{i,G+1}) < f(X_{i,G}) \\ X_{i,G} & otherwise. \end{cases} \tag{14}$$

where $i \in [1, N_P]$.

The flowchart of DE algorithm employed in the present study is shown in Fig. 6.

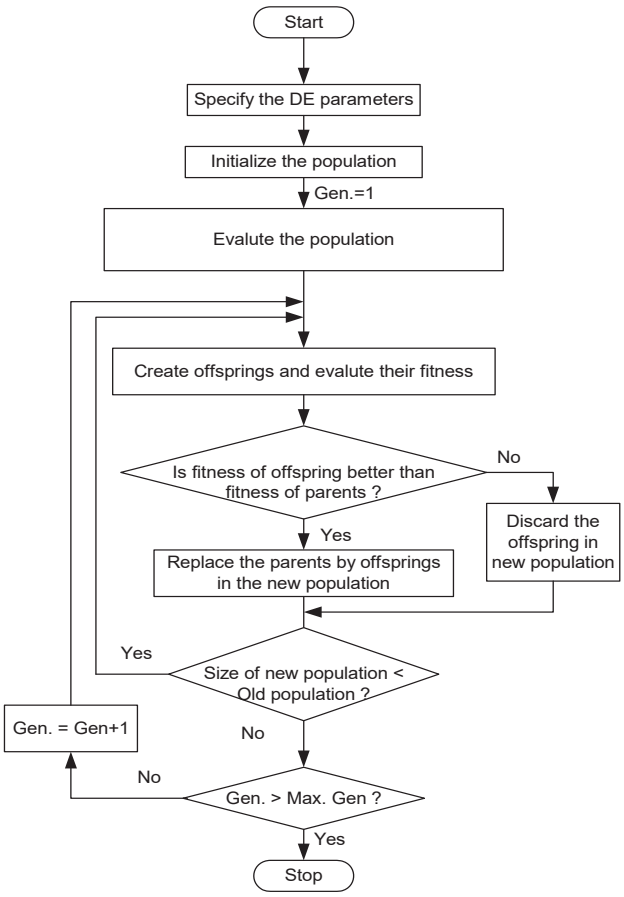

Fig. 6 Flow chart of DE

V. Results and Discussion

A. Implementation of PSO, BFO and DE Algorithm

The model of the system under study has been developed in MATLAB/Simulink environment and PSO, BFOA and DE program has been written (in .mfile). The developed model is simulated in a separate program (by .m file using initial population/controller parameters) considering a 1% SLP in area 2. The objective function is calculated in the .m file and

used in the optimization algorithms. The process is repeated for each individual in the population.

In this paper, the following PSO parameters are considered to verify the performance of the PSO optimized I /PI controller. Population size: 50; ω =0.9; c1=0.12; c2=0.12; Iteration: 60; For the efficient performance of BFOA, these parameters are selected carefully. In the present study, based on the previous experience S= 6, N_C = 4, N_S =5, N_{re}=7, N_{ed} =4, P_b =0.25, d_{at} =0.01, w_{at} =0.006, h_{re}= 0.03, w_{re}=12.

In the present study, a population size of N_P=50, generation number G=100, step size F=0.8 and crossover probability of CR =0.8 have been used. The strategy employed is: DE/best/1/exp.

TABLE I
CONTROLLER PARAMETERS

controller parameters			PSO tuned	BFOA tuned	DE tuned
PI controller	Proportional gain	K_{P1}	0.0093	0.0694	0.0783
		K_{P2}	0.9971	1.9306	0.8939
	Integral gain	K_{I1}	0.0295	0.0792	0.0295
		K_{I2}	0.0397	0.0438	0.03377
PID controller	Proportional gain	K_{P1}	0.5582	0.6584	0.3994
		K_{P2}	0.9945	1.250	0.9995
	Integral gain	K_{I1}	0.071	0.1190	0.063
		K_{I2}	0.035	0.04	0.0335
	Derivative gain	K_{D1}	0.3202	0.502	0.2522
		K_{D2}	2.2993	1.693	2.6994

Here, the upper and lower bounds of the gains are chosen as 3 and 0 respectively. Simulations were conducted on an Intel, core-2 Duo CPU of 2.4 GHz and 2MB RAM based computer in the MATLAB 7.10.0.499 (R2010a) environment. The optimization was repeated 20 times and the best final solution among the 20 runs is chosen as proposed controller parameters which are given in Table I.

B. Analysis of Results

A 1% SLP in area-2 is considered at t = 0 sec. The ITAE and settling times (2% of final value) of frequency and tie line power deviations with PSO, BFOA and the proposed DE optimized PI and PID controller are given in Table II for the system. To show the superiority of the proposed approach, the results are compared with a recently published approach (FLC) for the same interconnected power system [13].

TABLE II
ERROR CRITERIA, SETTLING TIMES, OVERSHOOT AND UNDERSHOOT WITH OBJECTIVE FUNCTION (J)

parameters		PSO tuned PI controller	PSO tuned PID controller	BFOA tuned PI controller	BFOA tuned PID controller	DE tuned PI controller	DE tuned PID controller	FLC controller [13]
ITAE		26.8964	19.1031	23.4719	18.4376	20.1239	18.4136	89.7002
T_S (sec)	Δf_1	115.34	95.03	115.28	79.11	107.27	64.59	136.95
	Δf_2	114.08	93.04	116.55	78.8	105.96	63.26	150
	ΔP_{Tie}	87.68	78.21	98.26	32.05	57.03	45.63	147

It is evident from Table III that with the proposed DE optimized PID and PI controllers; ITAE is improved by 79.47% and 77.57% respectively for PID and PI controller as compared to FLC. In case of PSO and BFO algorithms; ITAE is improved as compared to FLC. But, less value is obtained in DE algorithm i.e. 18.4136. The improvements in settling time of Δf_1 are 52.84% and 7.07%, respectively, for PID and PI controller as compared to FLC for DE algorithm. Similarly, settling time of Δf_1 is improved by 30.61% and 42.23%, respectively, with PSO and BFOA tuned PID controller as compared to FLC. The improvements in settling time of Δf_2 69.59% and 29.36%, respectively, for PID and PI controllers for DE algorithm. Similarly, setting time of Δf_2 is improved by 37.97% and 47.47%, respectively, with PSO and BFOA tuned PID controller. ΔP_{tie} also shows an improvement in settling time of 60.22% and 61.2%, respectively, for PID and PI controllers for DE algorithm.

Dynamic performances of area control error (ACE), frequency deviations and tie line power deviation responses of the system for a 1% SLP in area-2 occurring at t = 0 sec are simulated by proposed PI and PID controllers and controllers [13] shown in Figs. 7-11 and Figs. 12-16, respectively. For both PI and PID controllers the performances of ΔACE of both control areas are improved compared to FLC. From Fig. 7, the overshoot of ΔACE_1 is improved and found to be 22.12% and 39.42% for PI controller tuned with PSO and DE algorithm, respectively. Similarly, from Fig. 8, the overshoot of ΔACE_2 is improved and found to be 14.71% and 79.41% for PSO and DE tuned PI controller, respectively as compared to FLC. From Figs. 9, 10, it is clearly seen that overshoot of Δf_1

and Δf_2 is improved by 8.69% and 7.35%, respectively, for DE optimized PI controller as compared to FLC [13]. But, with PSO and BFOA tuned PI controller, no improvement is observed in case of the overshoot of Δf_1 and Δf_2. From Fig.11, the overshoot of tie line power deviation is improved with PSO, BFOA and DE tuned PI controller as compared to FLC. It is clearly understood from Fig. 12, that the overshoot of ΔACE_1 is improved by 48.75%, 72.12% and 38.46% with DE, PSO and BFOA optimized PID controller, respectively.

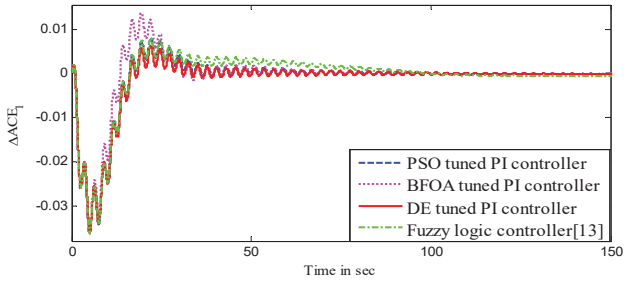

Fig. 7 Area control error of area-1 for step load change of 1% in area-2

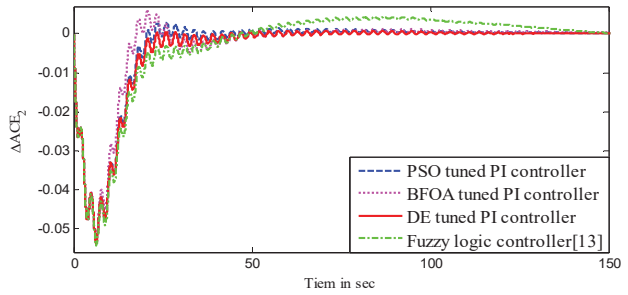

Fig. 8 Area control error of area-2 for step load change of 1% in area-2

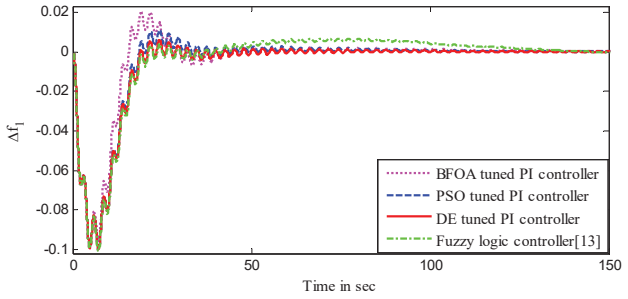

Fig. 9 Frequency deviation of area-1 for step load change of 1% in area-2

From Fig. 13, the overshoot of ΔACE_2 is improved by 93.02%, 79.14% and 55.88%, respectively, for DE, PSO and BFOA optimized PID controller as compared to the FLC [13]. From Fig. 14, it is observed that overshoot of Δf_1 is improved by 73.13%, 92.55% and 13.83%, respectively for PID controller tuned with DE, PSO and BFOA techniques. From Fig. 15, the overshoot of Δf_2 is improved by 72.06%, 92.78% and 10.31% respectively, DE, PSO and BFOA optimized PID controller as compared to FLC [13]. For the same contingency the tie line power deviation is shown in Fig. 16. It is seen from Fig. 16, both the overshoots and undershoots of DE, PSO and BFOA optimized PID controllers are improved as compared to FLC.

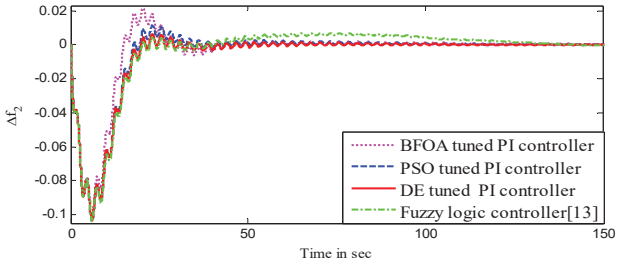

Fig. 10 Frequency deviation of area-2 for load change of 1% in area-2

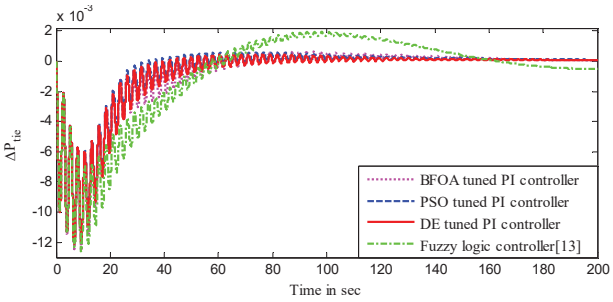

Fig. 11 Change in tie-line power for load change of 1% in area-2

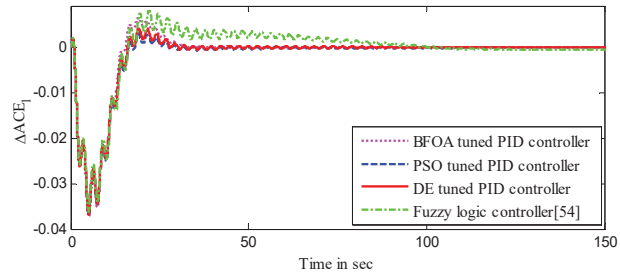

Fig. 12 Area control error of area-1 for step load change of 1% in area-2

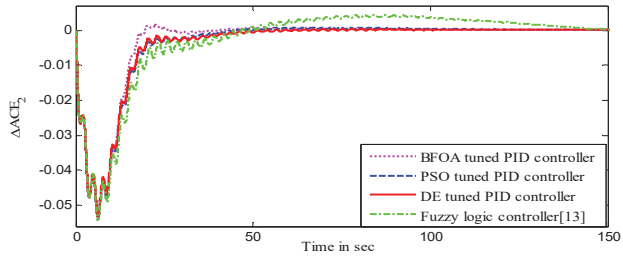

Fig. 13 Area control error of area-2 for step load change of 1% in area-2

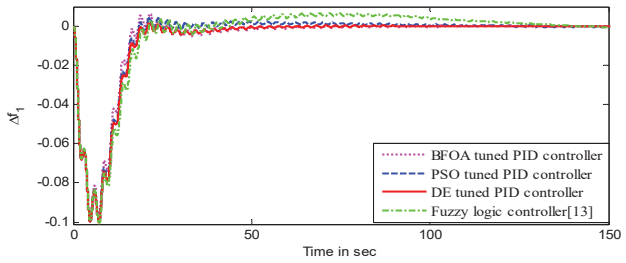

Fig. 14 Frequency deviation of area-1 for step load change of 1% in area-2

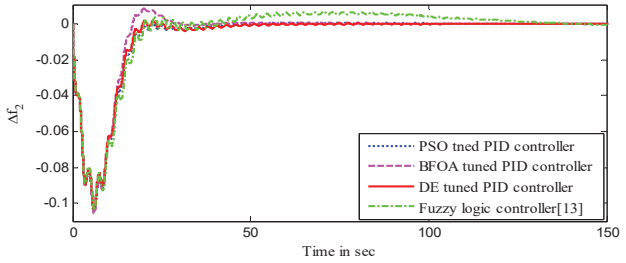

Fig. 15 Frequency deviation of area-1 for step load change of 1% in area-2

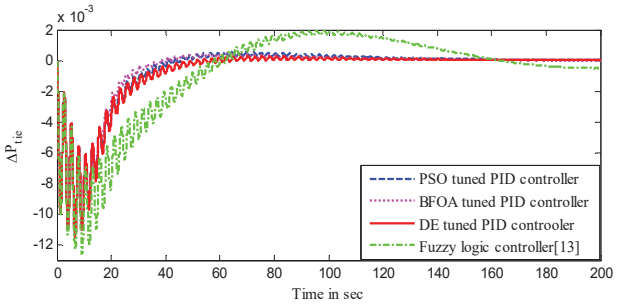

Fig. 16 Change in tie-line power for load change of 1% in area-2

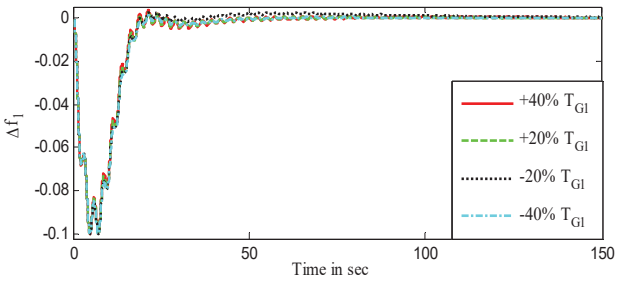

Fig. 17 Frequency deviation of area-1 for step load change of 1% in area-2 with variation in T_{G1}

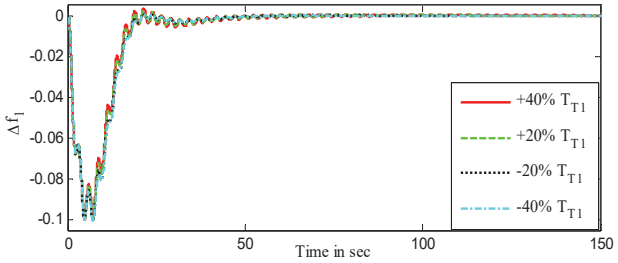

Fig. 18 Frequency deviation of area-1 for load change of 1% in area-2 with variation in T_{T1}

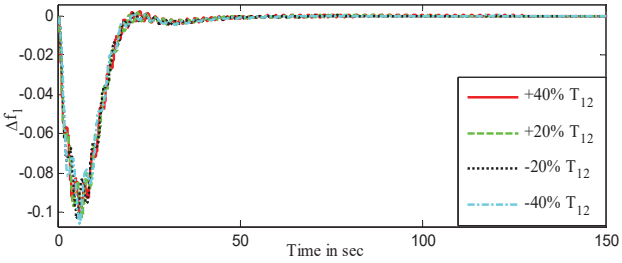

Fig. 19 Frequency deviation in area-1 for step load change of 1% in area-2 with variation in T_{12}

TABLE III
SENSITIVITY ANALYSIS

Parameter variation	% change	ISE	ITAE	ITSE	IAE	Settling time		
						Δf_1	Δf_2	ΔP_{tie}
T_{G1}	+40%	0.1368	18.8612	0.9411	1.8978	103.0	98.9	50.71
	+20%	0.1387	18.5976	0.9589	1.9132	69.66	68.2	48.09
	-40%	0.1378	20.2373	0.9465	1.9131	64.95	66.05	50.93
	-20%	0.142	18.4817	0.993	1.9443	59.79	58.52	43.27
T_{T1}	+40%	0.1322	18.7403	0.9084	1.8653	108.52	101.72	53.44
	+20%	0.1367	18.4267	0.9405	1.8951	72.32	68.35	48.27
	-40%	0.146	19.1162	1.0308	1.9819	54.82	55.97	40.76
	-20%	0.1435	18.6963	1.0063	1.957	59.62	58.29	43.07
T_{12}	+40%	0.1425	19.6926	1.0009	1.9956	96.28	88.25	47.31
	+20%	0.1414	19.055	0.9883	1.9436	66.09	64.81	46.34
	-40%	0.1388	26.1097	0.9543	1.9537	63.3	61.68	45.52
	-20%	0.1396	18.1352	0.966	1.9181	63.5	62	45.14

Especially, the overshoot of tie line power deviation is improved by 98.43%, 96.85% and 96.06%, respectively, with DE, PSO and BFOA optimized PID controller as compared to the published result of FLC [13]. As, PID controller tuned with DE algorithm gives better response than PI controller and other two algorithms, so PID controller tuned with DE is considered for further analysis.

To study the robustness of the proposed PID controller obtained by optimizing *J*, variations in the system parameters are deliberately introduced. For testing the controller

performance with parameter variations, governor time constants and turbine time constants of both the areas and the synchronizing power coefficient are varied in the range of *-40%* to *+40%* from their respective nominal values in steps of 20%. At each of these changed operating points, further 1% perturbation was introduced at area-2. The results of the sensitivity analysis obtained are provided in Table III.

The frequency deviations are obtained with the variation of turbine, governor and synchronizing time constants. The dynamics of system remain only marginally affected. These responses are highlighted in Figs. 17-19. It can be demonstrated from these figures that there is negligible effect of the variation of system time constants on the frequency deviation responses with the controller parameters obtained at nominal values. So, it can be concluded that, the proposed control strategy provides a robust and stable control satisfactorily. However, the optimum values of the proposed controller need not be reset for wide changes in the system parameters for the nominal loading.

VI. Conclusion

This paper presents the design and performance evaluation of PSO, BFOA and DE optimised PID and PI controllers for nonlinear AGC system considering boiler dynamics, GDB and GRCs. The dynamic performances of the proposed controllers with PSO, BFOA and DE are compared with FLC for the same system under study. The frequency deviation of areas and tie line power deviation responses are studied for 1% SLP in area-2. The proposed DE optimized PI and PID controllers able to provide better responses for frequency deviation and tie line power deviation with relatively smaller peak overshoot and lesser settling time as compared to PSO , BFOA and FLC. Further, the sensitivity analysis is carried out, which demonstrates the robustness of the proposed DE optimized PID controller to wide variations in system parameters.

Appendix

All the notations carry the usual meanings

Nominal system parameters of two-area hydro-thermal system with boiler dynamics, GDB and GRC:

$$B_1 = B_2 = 0.425 \text{p.u.MW/Hz}; R_1 = R_2 = 2.4 \text{Hz/p.u.}; T_{G1} = 0.2 \text{s};$$

$$T_{T1} = 0.3 \text{s}; T_{G2} = 48.7 s; T_1 = 0.513 s; T_2 = 10 s;$$

$$T_w = 1 \text{s}; T_r = 10 s; K_r = 0.333;$$

$$K_{PS1} = K_{PS2} = 120 \text{Hz/p.u.MW}; T_{P1} = T_{P2} = 20 \text{s}; T_{12} = 0.0707$$

$$\text{pu}; a_{12} = -1.$$

Boiler Data

$$K_1 = 0.85, K_2 = 0.095, K_3 = 0.92, c_b = 200, T_d = 0, T_f = 10 \text{s},$$

$$k_{ib} = 0.03, T_{ib} = 26 \text{s}, T_{rb} = 69 \text{s}.$$

References

[1] M. L Kothari., B. L Kaul., J Nanda, "*Automatic generation control of hydrothermal system*", Journal of Inst. of Engg. (India), vol. 61(2), Oct. 1980, pp. 85–91.

[2] J Nanda and A. Mangla, "*Some new findings on automatic generation control of an Interconnected Hydrothermal system with conventional controllers*", IEEE transaction on energy conversion Vol. 21(1), March 2006, pp187-194.

[3] J. Nanda, S. Mishra and L. C. Saikia, "*Maiden Application of Bacteria foraging-based optimization technique in Multi-area Automatic generation control*", IEEE Transactions on power systems, Vol.24, (2), May 2009, pp.602-609.

[4] H.Gozde and M. C. Taplamacioglu, "*Automatic generation control application with craziness based particle swarm optimization in a thermal power system*" Electrical power and energy systems, vol. 33,2011, pp. 8–16.

[5] R.R. Shoults and J.A. Jativa Ibarra, "*Multi area adaptive LFC developed for a comprehensive AGC simulation*", IEEE Transaction Power System, vol. 8 (2), 1993, pp 541–547.

[6] D. K. Chaturvedi, P. S. Satsangi, and P. K. Kalra, "*Load frequency control: A generalized neural network approach*", Electric power energy system, vol. 21, 6, Aug. 1999. pp. 405–415.

[7] S.P. Ghoshal, "*Optimizations of PID gains by particle swarm optimizations in fuzzy based automatic generation control*", Electric power systems research, vol. 72, 2004, pp. 203–212

[8] T.P.I Ahamed, P.S.N Rao and P.S Sastry, "*A reinforcement learning approach to automatic generation control"*, Electric Power System Research, vol. 63, 2002, pp. 9–26.

[9] S. R. Khuntia, and S. Panda, "*Simulation study for automatic generation control of a multi-area power system by ANFIS approach*", Applied Soft Computing, vol.12, 2012, pp. 333–341.

[10] J Nanda and A. Mangla, "*Some new findings on automatic generation control of an Interconnected Hydrothermal system with conventional controllers*", IEEE transaction on energy conversion Vol. 21(1), March 2006, pp187-194.

[11] J. Nanda, S. Mishra and L. C. Saikia, "*Maiden Application of Bacteria foraging-based optimization technique in Multi-area Automatic generation control*", IEEE Transactions on power systems, Vol.24, (2), May 2009, pp.602-609.

[12] U.K. Rout, R.K Sahu and S. Panda, "*Design and analysis of differential evolution algorithm based automatic generation control for interconnected power system*", Ain Shams Engg Journal, Vol.4(3), 2013, pp. 409-421.

[13] B. Anand and A. E Jayekumar, "*Fuzzy logic based load frequency control of hydro-thermal system with nonlinearities*", International journal of Electrical and Power Engineering, vol.3 (2), 2009, pp 112-118.

[14] "PSO Tutorial", available at: http://www.swarmintelligence.org/tutorials.php

[15] K.M. Passino, "*Biomimicry of bacterial foraging for distributed optimization and control*", IEEE Control Systems Magazine. Vol.22, 2002, pp. 52–67.

[16] S. Mishra, "*A hybrid least square-fuzzy bacterial foraging strategy for harmonic estimation*", IEEE Transaction evolution Comp. vol.9, 2005, pp. 61–73.

[17] R. Stron and K. Price, "*Differential evolution – A simple and efficient adaptive scheme for global optimization over continuous spaces*", Journal of Global Optimization, vol.11, 1995, pp.341-359.

[18] S. Das and P.N. Suganthan, "*Differential Evolution: A Survey of the State-of-the-Art*", IEEE transaction Evolution Compt., vol.15, 2011, pp.4-31.

Banaja Mohanty is a lecturer at Veer Surendra Sai University of Technology. Burla. Odissa. She is continuing Ph.D at VSSUT, Burla. M.E. degree in Electrical Engineering with specialization in Power Systems Engineering from University College of Engineering, Burla, Sambalpur University, B.Tech in Electrical Engineering from C.E.T, BBSR

Prakash Kumar Hota he is a professor in VSSUT, Burla. He had his graduation in Electrical and Electronics Engineering from the National Institute of Technology (NIT), Tiruchillapali, India in 1985. After a brief stint in private sector joined as lecturer in the Department of Electrical Engineering

of University College of Engineering Burla, Orissa in 1988 and became Reader in 1997 and also Professor in Training & placement of UCE Burla in 2006. He has been selected to be listed in "The Contemporary WHO's WHO" 2002-2003 published by The American Biographical Institute, USA on the basis of merited accomplishment and success in contemporary Society. He received the "Pandit Madan Mohan Malaviya award" by IE, India, "Rajlaxmi Memorial best engineering college teacher award by ISTE, New-Delhi" and "Union Ministry of Power, Department of power prize" for his outstanding contribution to Engineering and Technology research. He was the Dean, Students Welfare in VSS University of Technology from 2009-2011. His research interests include economic emission load dispatch, Hydrothermal Scheduling, Wind power generation, Power Quality and soft computing applications to different power system problems in deregulated environment.